



Published in final edited form as:

Oncogene. 2016 September 29; 35(39): 5191–5201. doi:10.1038/onc.2016.56.

Akt regulates Progesterone Receptor B dependent transcription and angiogenesis in endometrial cancer cells

Irene I. Lee¹, Kruti Maniar², John P. Lydon³, and J. Julie Kim¹

¹Division of Reproductive Science in Medicine, Department of Obstetrics and Gynecology, Robert H. Lurie Comprehensive Cancer Center, Northwestern University Feinberg School of Medicine, Chicago, IL, USA

²Department of Pathology, Northwestern University Feinberg School of Medicine, Chicago, IL, USA

³Department of Molecular and Cellular Biology, Baylor College of Medicine, Houston, TX, USA

Abstract

Progestins have long been used clinically for the treatment of endometrial cancers, however, the response rates to progestin therapy vary and the molecular mechanisms behind progestin insensitivity are poorly understood. We hypothesized that in *PTEN* mutated endometrial cancers, hyperactive Akt signaling downregulates Progesterone Receptor B (PRB) transcriptional activity, leading to overall impaired progestin responses. We report that inhibition of Akt with the Akt inhibitor, MK-2206 (MK), in conjunction with progestin (R5020) treatment, is sufficient to upregulate a subset of PRB target genes in Ishikawa cells stably expressing PRB (PRB-Ishikawa). Through gene ontology analysis of Akt-regulated PRB target genes, angiogenesis was found to be the principle process regulated by Akt-PRB. To further interrogate the mechanism by which Akt modulates PRB transcriptional activity, ChIP-Mass Spectrometry was performed to identify potential cofactors that differentially interact with PRB in the presence of the R5020 and MK +R5020. 14-3-3 σ was identified as a protein enriched in the MK+R5020 dataset, and it was demonstrated that 14-3-3 σ is required for the upregulation in PRB target gene expression following inhibition of Akt. In order to determine the ramifications of MK+R5020 treatment on angiogenesis, *in vitro* assays were performed and combinatorial MK+R5020 treatment significantly decreased endothelial cell invasion and tube formation more than MK or R5020 treatment alone. Furthermore, we found that combinatorial MK-2206+Progesterone treatments decreased angiogenesis and proliferation in the *Pten*^{d/d} conditional mouse model of endometrial cancer. Taken together, these findings suggest that a combinatorial therapeutic approach utilizing Akt inhibitors with progestins may improve the efficacy of progestin therapy for the treatment of endometrial cancer.

Users may view, print, copy, and download text and data-mine the content in such documents, for the purposes of academic research, subject always to the full Conditions of use: http://www.nature.com/authors/editorial_policies/license.html#terms

Corresponding Author: J. Julie Kim, 303 E. Superior St. Lurie 4-117, Chicago, IL 60611. Phone: (312) 503-5377, Fax: (312) 503-0095, j-kim4@northwestern.edu.

Conflict of Interest: The authors disclose no potential conflicts of interest.

Keywords

endometrial cancer; progesterone; Akt; angiogenesis; 14-3-3

Introduction

Endometrial cancer is the fourth most commonly diagnosed cancer in women; NCI estimates approximately 54,870 new cases in the United States in 2015.¹ Type I endometrial carcinomas, are estrogen and progesterone receptor positive, and are associated with chronic estrogen exposure and insufficient countering progesterone.² Total abdominal hysterectomy with bilateral oophorectomy is currently considered the standard of care for type I endometrial carcinoma. However, primary progestin therapy may be considered for reproductive-aged women with early stage well differentiated disease, in cases where surgery is not an option, or in recurrent or advanced endometrial cancers. Comprehensive meta-analysis studies suggest that approximately 76% of early stage low-grade endometrial cancer cases treated with progestins demonstrated a complete response.^{3, 4} While patients respond well initially to progestin, 24–47% of cases develop recurrence.^{3–6} In cases of advanced or recurrent endometrial cancer, only 16–25% demonstrated a response to progestin therapy.⁷ Additionally, there is no current clinical standard protocol regarding the type, dose, or duration for progestin therapy, further complicating our understanding of the effectiveness of progestins in the treatment of endometrial cancer. It is clear that improvements are needed in the use of progestin therapy. The effects of progestins are mediated primarily through its receptor, Progesterone Receptor (PR). PR belongs to the family of steroid hormone receptors that act as transcription factors upon ligand binding. PR regulates genes involved in cell adhesion, invasion, apoptosis, proliferation, cell cycle regulation, inflammation, and differentiation and is considered one of the predominant tumor suppressors in the endometrium.⁸ PR has two main isoforms, PRA and PRB; PRB is the full-length form that has an additional 164 amino acids at the N-terminus that contains an additional transactivation function (AF3). The specific roles of PRA and PRB in endometrial cancer remain unclear, however, in vitro studies suggest that PRB may be the predominant isoform responsible for the tumor suppressive action of progesterone in the endometrium.^{9–11}

The causative molecular mechanisms underlying progestin insensitivity in endometrial cancer have yet to be determined. However, recent evidence has implicated a putative role for PI3K/Akt in the promotion of progestin resistance in endometrial cancer. Akt is found to be overactive in the majority of endometrial cancers; recent sequencing analysis for the Cancer Genome Atlas has determined that greater than 90% of endometrioid endometrial tumors have some genetic aberration in the PTEN/PI3K pathway, leading to increased Akt activity.¹² We and others have shown that combinatorial PI3K/Akt inhibitor and progestin treatment can synergize to decrease endometrial cancer cell viability as well as decrease xenograft growth.^{13, 14} Furthermore, it has been shown that inhibition of PI3K/Akt signaling reversed progestin resistance through a PR-dependent non-genomic rapid signaling mechanism.¹³ However, the consequences of overactive Akt signaling on the genomic function of PR have yet to be explored. In this study, we hypothesized that Akt directly

causes progesterin insensitivity in endometrial cancer through the downregulation of PRB transcriptional activity. Here, we show that inhibition of hyperactive Akt signaling is sufficient to upregulate the transcription of PRB target genes and that the novel cofactor, 14-3-3 σ , is required for this upregulation in PRB transcriptional activity. Finally, we report that combinatorial progesterin and Akt inhibition treatments can decrease angiogenesis in both endometrial cancer cells as well as in a mouse model of endometrial cancer.

Results

Knockdown or inhibition of Akt activity upregulates PRB transcriptional activity

In order to investigate the relationship between PR and Akt, we first examined the effects of inhibition of Akt on PRB-dependent transcription in Ishikawa cells that stably express PRB and overexpress phospho-Akt as a result of a PTEN-inactivating mutation.¹¹ The PRB-Ishikawa cells were treated with non-silencing control siRNAs (siCtrl) or a pool of Akt-specific siRNAs (siAkt) in the absence or presence of the progesterin, R5020, for 24 hours. Microarray analysis was performed and differentially expressed genes were identified for each treatment group. Approximately 113 differentially expressed genes were identified in the siAkt + R5020 treatment group when compared to the siAkt Vehicle Control (VC) and siCtrl R5020 groups (Figure 1A–B, Supplementary Tables 1–3). Gene ontology analysis led to the identification of a number of classical progesterone regulated pathways, including cell adhesion and cell proliferation (Figure 1C). The leading scoring process enriched in the siAkt R5020 group was determined to be angiogenesis regulation. Real-time PCR analysis of both previously established and novel PRB target genes revealed that a subset of PRB target genes were further upregulated upon knockdown of Akt (Figure 1D). We confirmed that knockdown of Akt significantly decreased protein expression of both phospho Akt (S473) and pan Akt (Figure 1E). These experiments were repeated utilizing the allosteric Akt inhibitor, MK-2206, which inhibits all three isoforms of Akt by reducing Akt activation¹⁴ (Figure 1G). Treatment with MK-2206 and R5020 resulted in the upregulation of all PRB target genes tested (Figure 1F), indicating that both inhibition and depletion of Akt are sufficient to increase PRB target gene expression.

In order to confirm the role of PRB, PRB expression was knocked down using siRNA, and then subsequently treated with Vehicle, MK-2206, R5020, or MK+R5020 for 24 hrs and then real-time PCR analysis was performed. The majority of PRB target genes were significantly downregulated upon PRB knockdown, indicating that these genes are dependent upon PRB (Figure 1H–I). Taken together, depletion or inhibition of Akt is sufficient to upregulate the expression of a subset of PRB target genes in a PRB-dependent manner.

Inhibition of Akt does not alter PRB genome-wide recruitment to chromatin

In order to determine the mechanism by which Akt downregulates PRB transcriptional function, PR ChIP-Seq was performed to interrogate how Akt influences PRB recruitment to its regulatory regions. PRB-Ishikawa cells were pre-treated with either DMSO or 1 μ M MK-2206 overnight and then subsequently treated with 10 nM R5020 for 30 minutes. ChIP-Seq was then performed to identify PRB genome-wide binding sites, and R5020 and MK

+R5020 datasets were compared. ChIP-Seq analysis indicated that there was no significant difference in PRB genome-wide recruitment between the R5020 and MK+R5020 treatments. Approximately 11,004 and 12,021 PRB binding sites were identified in the R5020 dataset and MK+R5020 dataset respectively, and only 102 binding sites demonstrated differential binding between the R5020 and MK+R5020 treatments. Tag density counts between the R5020 and MK+R5020 datasets were graphed and the majority of data points were located near the $y=x$ line, indicating a high degree of similarity between datasets (Figure 2A). Closer examination of PRB regulatory regions at select PRB target genes (*PDK4*, *TIPARP*) that are upregulated in response to Akt inhibition, demonstrated no appreciable difference in either signal or binding site location (Figure 2B). Similar to what has been previously reported in breast cancer cells,¹⁵ the vast majority of PRB binding sites were located within enhancer regions. In both the R5020 and MK+R5020 datasets, approximately 48% of PRB binding sites were located within intronic regions, 37% in intergenic regions, and 8% found in promoter regions. Additionally, there was no significant difference in PRB binding site location between the R5020 and MK+R5020 treatments (Figure 2C). Finally, HOMER motif analysis indicated similarly enriched binding motifs between the R5020 and MK+R5020 treatments, identifying PRE, GRE, ARE, and AP-1 binding motifs as the most significant (Table 1). From the ChIP-Seq analysis, we concluded that inhibition of Akt does not directly upregulate PRB genome-wide binding.

ChIP-Mass Spectrometry Analysis identifies 14-3-3 σ is required for the induction in PRB target genes following Akt inhibition

After establishing that inhibition of Akt is sufficient to upregulate the expression of PRB target genes, but does not alter PRB genome-wide binding, we hypothesized that Akt may influence cofactors of PRB in order to modulate PRB transcriptional activity. To identify these cofactors of PRB that are influenced by inhibition of Akt, ChIP followed by Mass Spectrometric analysis of PRB interacting proteins was performed. This method termed RIME has been previously implemented to successfully identify ER cofactors.¹⁶ Upon mass spectrometric analysis, stringent criteria were applied to further filter identified proteins: any protein identified in the IgG-control sample was excluded, only PRB-associated proteins present in both duplicates were included, and a Peptide Spectrum Match (PSM) cutoff of 3 was implemented. From this analysis, 21 proteins were identified in the R5020 dataset and 315 proteins in the MK+R5020 dataset (Figure 3A, Supplementary Table 4–5). There were 295 proteins identified in the MK+R5020 dataset that were distinct from the R5020 dataset. PR was identified in both the R5020 and MK+R5020 datasets as one of the top scoring proteins. Gene ontology analysis indicated that the majority of proteins identified in the R5020 dataset are involved in protein and nucleic acid binding (Figure 3B). Similarly, the MK+R5020 dataset also featured a number of proteins involved in protein and nucleic acid binding, but also included proteins involved in regulating catalytic function and transcription factor activity. Gene pathway enrichment analysis on the 295 unique proteins in the MK+R5020 dataset indicated that the 14-3-3 pathway was the most significantly enriched pathway in the MK+R5020 dataset (Figure 3C). Six out of the seven 14-3-3 family members were found in the MK+R5020 dataset, while none were identified in the R5020 dataset (Figure 3D). To determine if 14-3-3 family members play a role in the Akt-dependent regulation of PRB transcriptional activity, each 14-3-3 member was knocked down in PRB-

Ishikawa cells and then treated with MK and R5020 for 24 hrs. Real-time PCR analysis on PRB target genes was then performed (data not shown). Of all the 14-3-3 isoforms, knockdown of the 14-3-3 σ isoform significantly attenuated the MK+R5020 upregulation in the majority of PRB target genes tested (Figure 3E). Knockdown of 14-3-3 σ significantly attenuated the MK+R5020 upregulation in PRB target genes but did not significantly attenuate the R5020 response, indicating that 14-3-3 σ is required for the Akt-dependent regulation of PRB transcriptional activity. Western blot analysis confirmed that 14-3-3 σ expression was decreased in si14-3-3 σ transfected cells (Figure 3F). We confirmed the interaction between 14-3-3 σ and PRB, through co-immunoprecipitation in PRB-Ishikawa nuclear extracts treated with Vehicle, MK, R5020, or MK+R5020 (Figure 3G). We utilized the parental Ishikawa cell line that expresses low levels of both PR and 14-3-3 σ as a negative control. Altogether, these findings indicate a putative and novel role for 14-3-3 σ in the Akt-dependent transcriptional regulation of PRB.

Combinatorial Akt inhibition and R5020 treatments further decrease angiogenesis in vitro

After establishing that hyperactive Akt activity is sufficient to inhibit PRB transcriptional activity, we then investigated the effects of combinatorial Akt inhibition and progestin treatment on angiogenesis which was previously identified as a key pathway regulated by siAkt + R5020 (Figure 1C). Real-time PCR analysis was performed on a number of angiogenesis-related genes discovered through microarray analysis and several were significantly upregulated (*AMOT*, *CTGF*, *F3*) or downregulated (*IDI*) in response to MK + R5020 treatment (Figure 4A). We then sought to explore the effects of combinatorial MK-2206 and R5020 treatment in *in vitro* angiogenesis assays. An endothelial cell invasion assay was performed, utilizing uterine microvascular endothelial cells (UtmVEC) and conditioned media from PRB-Ishikawa cells treated with either Vehicle, MK, R5020, or MK + R5020 for 24 hrs. Endothelial cell invasion is an early step in the angiogenesis process, and is required in order for endothelial cells to proliferate.¹⁷ The combination of MK-2206 and R5020 significantly decreased endothelial cell invasion more than any of the other treatments alone (Figure 4B). Additionally, an endothelial tube formation assay was performed to determine how MK-2206 and R5020 treatments might influence endothelial network formation on a basement membrane matrix. PRB-Ishikawa cells were treated with Vehicle, MK, R5020, or MK + R5020 for 24 hrs and the conditioned media was collected and then incubated with UtmVEC plated on a basement membrane matrix. MK + R5020 treatment significantly decreased the number of branching points formed more than any of the other treatments alone (Figure 4C). To ensure that the effects observed on both endothelial invasion and tube formation were not due to the MK-2206 and R5020 having direct effects on the viability of the endothelial cells, a WST cell viability assay was performed. The WST assay demonstrated no differences between any of the treatment groups, indicating that the MK-2206 and R5020 were not acting directly to decrease the cell viability of the endothelial cells (Figure 4D). Altogether, we concluded that angiogenesis is a process regulated by the Akt-PR relationship.

Combinatorial MK-2206 and Progesterone treatments further decrease angiogenesis and proliferation in a conditional *Pten*^{d/d} mouse model

To extend our *in vitro* findings to a physiologically relevant model, we examined the effects of MK and progesterone in the *Pten*^{d/d} endometrial cancer mouse model. In this mouse model, *Pten* is conditionally deleted from the endometrium; these mice develop carcinoma *in situ* within one month and carcinoma with myometrial invasion within three months.¹⁸ Three-month-old mice were separated into four treatment groups: Vehicle, MK-2206, Progesterone (P4), and MK+P4 (Figure 5A). Treatments were carried out for six weeks and then mice were sacrificed and the uteri were measured and harvested. Gross uterine weight was decreased in the MK+P4 treatment group, but this decrease in weight was not statistically significant (Figure 5B). H&E staining was performed to determine the progression of endometrial cancer in each treatment group. H&E stained slides were examined and scored by a pathologist according to FIGO guidelines for endometrial cancer grading (Figure 5C). All nine of the Vehicle mice had grade 1 endometrioid endometrial cancer (Table 2). Interestingly, four out of ten MK+P4 mice demonstrated benign squamous metaplasia with no evidence of endometrial cancer, potentially indicating a role for MK+P4 in endometrial cancer progression. We additionally stained for both PR and 14-3-3 σ , however, their expression did not significantly change with MK, P4, or MK+P4 treatment (Supplementary Figure 1).

In order to determine the extent of angiogenesis in each treatment group, IHC staining for the endothelial cell marker, CD31, was performed. The MK+P4 treatment group demonstrated significantly decreased CD31 positive blood vessel staining when compared to the Vehicle treatment group (Figure 5D). However, the MK+P4 treatment group did not demonstrate a statistically significant difference in CD31 staining when compared to either the MK or P4 treatment groups. Ki67 staining was also performed to investigate how cell proliferation was affected by MK+P4 treatment (Figure 5E). The MK+P4 treatment group demonstrated significantly decreased Ki67 positive epithelial cells when compared to the Vehicle, MK-2206, and P4 treatment groups. While gross uterine weight was not decreased in the MK+P4 treatment group, we observed decreased CD31 and Ki67 staining, potentially indicating that the combinatorial MK+P4 treatment has antiangiogenic and antiproliferative effects in the *Pten*^{d/d} endometrial cancer mouse model.

Discussion

Although progestin therapy has been used clinically for decades, the molecular mechanisms underlying progestin insensitivity in endometrial cancer are poorly understood. Given the prevalence of PI3K/Akt mutations in endometrial cancer, we proposed that overactive Akt is responsible for rendering endometrial cancer cells insensitive to progestin. In this study, we demonstrated that inhibition of Akt is sufficient to upregulate the transcriptional activity of Progesterone Receptor B in endometrial cancer cells. Previous evidence indicated that inhibition of PI3K/Akt may reverse progestin resistance through the attenuation of non-genomic progestin-mediated re-activation of the PI3K/Akt pathway.¹³ In contrast to what was previously shown, our work demonstrates that Akt regulates PRB genomic function in endometrial cancer. In our study, we identified a specific subset of PRB target genes that

were modulated upon knockdown or inhibition of Akt. However, ChIP-Seq analysis indicated that inhibition of Akt does not alter PRB genome-wide binding. We utilized a short 30-minute time point in this study, and it is possible that inhibition of Akt may affect PRB recruitment to its target genes at later time points. PR ChIP-Seq has been performed previously in breast cancer and in mouse uterine tissue;^{15, 19} however, this is the first report of PRB specific ChIP-Seq in endometrial cancer, and the first to examine the effects of an Akt inhibitor on PRB genome-wide recruitment. We identified AP1 and NF1 binding motifs enriched near PRB binding regions, consistent with what has been previously reported in the mouse uterus and in the AB32 normal breast cancer cell line. However, in contrast with what has been reported in T47D breast cancer cells, we did not identify FOXA1 motifs enriched near PRB binding regions, nor was FOXA1 identified in either the R5020 or MK+R5020 ChIP-mass spectrometry datasets. Additionally, the Akt substrate and PR cofactor, FOXO1, was not identified in either the ChIP-Seq and ChIP-mass spectrometry datasets. FOXO1 has been shown to cooperate with PR during the decidualization process in endometrial stromal cells;^{20, 21} however, its expression is significantly downregulated in Ishikawa cells and in primary endometrial cancer tissue.²² In our study, we have identified a potential PR transcriptional regulatory mechanism that appears to be FOXO1 independent; these findings may further indicate that PR binding is both tissue and context specific, with a range of diverse cofactors involved in the regulation of PR transcriptional activity.

We identified 14-3-3 σ as a required mediator in the Akt-dependent regulation of PRB transcriptional activity. 14-3-3 proteins are a highly conserved protein family found to be critical mediators of signal transduction, cell cycle regulation, and transcriptional regulation. 14-3-3 proteins bind as dimers and recognize specific phosphoserine or phosphothreonine motifs, although their interaction can also occur in a phosphorylation independent manner.²³ While not considered classical cofactors of steroid hormone receptors, 14-3-3 proteins have been previously implicated in the regulation of AR, ER, and GR. Overexpression of 14-3-3 is sufficient to enhance the transcriptional activity of both AR and GR.²⁴⁻²⁶ Additionally, 14-3-3 has been shown to interact with known nuclear receptor cofactors RIP140, TRAP220, ACTR; in the case of RIP140, 14-3-3 has been demonstrated to alter RIP140 nuclear localization and thus relieve inhibition upon GR transactivation.²⁷ Finally, recent findings have indicated that ER α and 14-3-3 interaction are sufficient to inhibit ER α dimerization, interaction with chromatin, and subsequent expression of its target genes.²⁸ While 14-3-3 is emerging as a potentially critical mediator in steroid hormone receptor function, to our knowledge, 14-3-3 σ has not been previously shown to play a role in the regulation of PRB transcriptional function. Although we identified six out of the seven 14-3-3 family members in our ChIP-Mass Spectrometry screen, only knockdown of the 14-3-3 σ isoform demonstrated significant decreases in PRB target gene expression. Of all the 14-3-3 isoforms, 14-3-3 σ is considered to be the isoform most associated with tumor suppression due to its loss of expression in many different types of cancer.^{29, 30} Furthermore, 14-3-3 σ expression is decreased in endometrial adenocarcinoma compared to the normal endometrium.^{30, 31} While 14-3-3's have long been associated with signal transduction and nuclear shuttling, its role as a direct transcriptional coactivator is still unclear. Recent evidence suggests that 14-3-3 proteins are required for transcriptional activation of certain genes due to its role as a detector for phosphorylated S10 of histone H3.³² It remains to be

determined whether 14-3-3 σ is acting as a direct transcriptional coactivator of PRB at the level of chromatin. Taken together, 14-3-3 σ may play an important role in regulating the tumor suppressive action of PRB in endometrial cancer.

Our findings also suggest that the Akt-PR relationship is actively involved in the regulation of angiogenesis in endometrial cancer. The endometrium is subject to complex cyclical changes in cellular proliferation, differentiation, vascular repair, and angiogenesis; these processes are largely governed by estrogen and progesterone. Estrogen appears to play a predominant role in the regulation of angiogenesis in the uterus by stimulating endothelial proliferation and migration, inducing expression of VEGF, and increasing recruitment of inflammatory cells to the uterus.^{33–35} However, the role of progesterone in endometrial angiogenesis remains unclear; a number of studies suggest that progesterone can both inhibit and increase angiogenesis in the uterus.^{36–38} Here, we demonstrated that with combinatorial MK+R5020 treatment in PRB-Ishikawa cells, this paracrine action decreased both endothelial cell invasion and tube formation *in vitro*. Given that the role of progesterone in the uterus is to oppose the effects of estrogen, it is possible that the combination of Akt inhibitors with progestins may oppose the angiogenesis stimulatory effects of estrogen in endometrial cancer. However, further investigation determining the precise mechanism by which Akt-PRB decreases angiogenesis is warranted.

Furthermore, we found that the combination of MK-2206 with P4 further decreased angiogenesis and proliferation in the *Pten^{d/d}* endometrial cancer mouse model, but did not significantly decrease uterine weight. Recent evidence has indicated a prominent role for PR in the regulation of vascular permeability that ultimately leads to physiological edema in the endometrium.³⁹ In our *Pten^{d/d}* endometrial cancer mouse model, we did not observe a significant difference in uterine weight and this observation may be explained by excessive swelling of the uterus caused by progesterone. We observed a trend towards increased uterine weight in the progesterone only treated group, and given the role of progesterone in mediating physiological edema, this result is not surprising. While the *Pten^{d/d}* endometrial cancer mouse model develops abnormal glands that resemble human endometrioid endometrial cancer, these mice also develop extensive squamous metaplasia, which may further complicate understanding how the MK and P4 treatments affect the glandular epithelium. Future studies may benefit from using an approach in which an epithelial specific, inducible *Pten^{ff}* mouse model is used to better mimic human disease.

In this study, our results demonstrate that inhibition of hyperactive Akt signaling is sufficient to upregulate PRB transcriptional function and decrease angiogenesis in endometrial cancer. We observed that 14-3-3 σ is a critical mediator of the Akt-dependent regulation of PRB transcriptional function. Taken together, our results suggest that a combinatorial Akt inhibitor and progestin treatment may be more effective than progestin therapy alone for the treatment of endometrial cancer.

Materials and Methods

Additional methods and details are provided in Supplementary Methods.

Cell Culture and Reagents

PRB-Ishikawa cells were generously provided by Dr. Leen Blok (Erasmus University, Netherlands).¹¹ These cells were maintained in DMEM/F12 supplemented with 10% FBS, sodium pyruvate, penicillin/streptomycin, hygromycin, and G418. PRB-Ishikawa cells were sequenced and authenticated by Dr. Christopher Korch at the University of Colorado Cancer Center (UCCC) DNA Sequencing & Analysis Core. Primary uterine microvascular endothelial cells were purchased from Lonza (Basel, Switzerland) and maintained in Endothelial Growth Media supplemented with 2% FBS, hEGF, VEGF, R3-IGF-1, Ascorbic Acid, Hydrocortisone, hFGF- β , Heparin, and GA. MK-2206 was generously provided by Merck Sharp & Dohme Corp (Kenilworth, NJ, USA) and the National Cancer Institute, National Institutes of Health (Bethesda, MD, USA).

Transfection and siRNA

PRB-Ishikawa cells were transfected with siRNA using Lipofectamine RNAiMax (Life Technologies, Grand Island, NY, USA) according to the manufacturer's instructions. ON-TARGETplus SmartPool non-targeting control siRNA, siAKT1, siAKT2, siAKT3, siPR, and siSFN were purchased from GE Dharmacon (Lafayette, CO, USA).

ChIP-Mass Spectrometry and ChIP-Seq

Chromatin Immunoprecipitation was performed utilizing the SimpleChIP Enzymatic Chromatin IP Kit (Cell Signaling, Danvers, MA, USA) according to the manufacturer's instructions. For further description, see Supplementary Methods.

RNA Extraction and Real-Time PCR

Cells were harvested for RNA extraction using Tri Reagent (Sigma Aldrich, St. Louis, MO, USA). RNA was then extracted using the Zymo Research (Irvine, CA, USA) Direct-zol RNA Extraction Kit according to the manufacturer's instructions. RNA samples were treated with DNase I (Zymo Research) to remove any contaminating DNA. First strand cDNA synthesis was then performed using 2 μ g of RNA and M-MLV reverse transcriptase (Life Technologies). Real-Time PCR was then performed using the following Taqman Primers: *FKBP5*, *MT2A*, *NET1*, *NFKBIA*, *PDK4*, *RASD1*, *RPLP0*, *SGK1*, *TBP*, *TIPARP* (Applied Biosystems/Life Technologies). SYBR-Green Primers were used for *AMOT*, *ANKRD1*, *BCL6*, *CTGF*, *CX3CL1*, *EFNB2*, *F3*, *IDI1*, *IL1R1*, *MT1X*, and *PPP1R1B*; primer sequences are listed in Supplementary Methods. Fold change values were calculated using the Ct method using *RPLP0* or *TBP* as housekeeping genes.⁴⁰

Microarray

PRB-Ishikawa cells were transfected with either siCtrl, or siAkt1, siAkt2, and siAkt3. Cells were then serum starved overnight and then subsequently treated with either Ethanol Vehicle or 10 nM R5020 for 24 hrs. For further description, see Supplementary Methods.

Cell Lysis and Immunoblotting

Cell lysis and western blotting was performed as previously described.^{14, 41} Membranes were probed with the following primary antibodies: phospho Akt S473 (#9271), pan-Akt

(#4691, Cell Signaling), β -Actin (#A1978, Sigma Aldrich), α -Tubulin (#05-829, Millipore, Billerica, MA, USA), PR (#SC-7208X, Santa Cruz, Santa Cruz, CA, USA), TBP (#ab818, Abcam), and 14-3-3 σ (#A301-648A, Bethyl Laboratories, Montgomery, TX, USA). Membranes were developed using ECL Reagents (Life Technologies) and protein bands were visualized with a Fuji Film LAS-3000 Imaging System (Stamford, CT, USA).

***Pten*^{d/d} Mouse Model and Treatments**

All mouse experiments were carried out in accordance with protocols approved by the Institutional Animal Care and Use Committees at Northwestern University. Mice were maintained in the animal care facility at the Center for Comparative Medicine at Northwestern University according to the institutional guidelines for the care and use of laboratory animals. *PR*^{Cre/+} and *Pten*^{f/f} mice were generously provided by Dr. John Lydon (Baylor College of Medicine, Houston, TX, USA).¹⁸ *PR*^{Cre/+} *Pten*^{f/f} (*Pten*^{d/d}) mice were generated by breeding *PR*^{Cre/+} mice with *Pten*^{f/f} mice. Genotyping was performed using genomic DNA extracted from tail biopsies and PCR was performed utilizing primers for *Cre* and *Pten*. In order to study the effects of combinatorial MK-2206 and Progesterone treatment, three month-old female *Pten*^{d/d} mice were given either Vehicle (30% Captisol, Ligand Pharmaceuticals, La Jolla, CA, USA), MK-2206 (Merck), Progesterone (5 mg/21-day pellet, Innovative Research of America, Sarasota, FL, USA), or MK-2206+Progesterone. Progesterone pellets were implanted subcutaneously and replaced with fresh pellets after three weeks of treatment. MK-2206 was dissolved in 30% Captisol at a dose of 120 mg/kg and administered by oral gavage two times per week. Mice were litter randomized in each treatment group, and investigators were not blinded to treatment groups. After six weeks of treatment, mice were sacrificed and uteri were harvested. Nine mice were used per group with the exception of the MK+P4 treatment group, which included ten mice.

Histology and Immunohistochemistry

Uterine tissues were fixed in formalin and then paraffin embedded. 5 μ m uterine sections were cut and mounted on charged histology glass slides. Sections were then stained with hematoxylin and eosin. H&E stained sections were scored by a pathologist according to the FIGO grading system. Immunohistochemistry was performed using the EnVision DAB Kit (Dako, Carpinteria, CA, USA) according to manufacturer's instructions. The following antibodies were used for immunohistochemistry: CD31 (#E1110, Spring Bioscience, Pleasanton, CA, USA) and Ki67 (#Ab15580, Abcam, Cambridge, MA, USA). CD31 staining was quantified by counting CD31+ blood vessels in six different 40X fields using ImageJ. Ki67 staining was quantified by counting Ki67+ epithelial cells in six different 40X fields using ImageJ.

Statistics

All statistical analysis was performed using Graphpad Prism version 6.0 (Graphpad Software, La Jolla, CA, USA). All data represent the mean \pm SEM of a minimum of three independent experiments and data were considered statistically significant if the p-value was < 0.05. For real-time PCR data, *in vitro* angiogenesis assays, and cell viability assays, paired student's t-tests were performed based on the assumption of a normal distribution and equal sample variance. For real-time PCR and cell viability assays, in which fold changes were

calculated, data were first log normalized in order to achieve a more normal distribution. For mouse studies, unpaired student's t-tests were performed. No exclusion of data points were used.

Supplementary Material

Refer to Web version on PubMed Central for supplementary material.

Acknowledgments

We would like to acknowledge the Northwestern Genomics Core Facility, the Northwestern Proteomics Core Facility, and the Northwestern Next Generation Sequencing Core Facility. We would also like to thank members of the Kim laboratory for technical assistance and insightful discussion and review of the manuscript. This work is supported by NIH/NCI training grant T32CA09560 (IIL), Malkin Scholars Program from the Robert H. Lurie Comprehensive Cancer Center of Northwestern University (IIL), NIH/NICHD grant R01HD042311 (JPL), and NIH/NCI grant R01CA155513 (JK).

References

1. Institute NC. SEER Stat Fact Sheets: Endometrial Cancer. 2015; 2015
2. Bansal N, Yendluri V, Wenham RM. The molecular biology of endometrial cancers and the implications for pathogenesis, classification, and targeted therapies. *Cancer Control*. 2009; 16:8–13. [PubMed: 19078924]
3. Erkanli S, Ayhan A. Fertility-sparing therapy in young women with endometrial cancer: 2010 update. *Int J Gynecol Cancer*. 2010; 20:1170–1187. [PubMed: 21495221]
4. Ramirez PT, Frumovitz M, Bodurka DC, Sun CC, Levenback C. Hormonal therapy for the management of grade 1 endometrial adenocarcinoma: a literature review. *Gynecol Oncol*. 2004; 95:133–138. [PubMed: 15385122]
5. Park JY, Nam JH. Progestins in the fertility-sparing treatment and retreatment of patients with primary and recurrent endometrial cancer. *The oncologist*. 2015; 20:270–278. [PubMed: 25673106]
6. Ushijima K, Yahata H, Yoshikawa H, Konishi I, Yasugi T, Saito T, et al. Multicenter phase II study of fertility-sparing treatment with medroxyprogesterone acetate for endometrial carcinoma and atypical hyperplasia in young women. *J Clin Oncol*. 2007; 25:2798–2803. [PubMed: 17602085]
7. Thigpen JT, Brady MF, Alvarez RD, Adelson MD, Homesley HD, Manetta A, et al. Oral medroxyprogesterone acetate in the treatment of advanced or recurrent endometrial carcinoma: a dose-response study by the Gynecologic Oncology Group. *J Clin Oncol*. 1999; 17:1736–1744. [PubMed: 10561210]
8. Yang S, Thiel KW, Leslie KK. Progesterone: the ultimate endometrial tumor suppressor. *Trends Endocrinol Metab*. 2011; 22:145–152. [PubMed: 21353793]
9. Dai D, Kumar NS, Wolf DM, Leslie KK. Molecular tools to reestablish progestin control of endometrial cancer cell proliferation. *Am J Obstet Gynecol*. 2001; 184:790–797. [PubMed: 11303185]
10. Dai D, Wolf DM, Litman ES, White MJ, Leslie KK. Progesterone inhibits human endometrial cancer cell growth and invasiveness: down-regulation of cellular adhesion molecules through progesterone B receptors. *Cancer research*. 2002; 62:881–886. [PubMed: 11830547]
11. Smid-Koopman E, Blok LJ, Kuhne LC, Burger CW, Helmerhorst TJ, Brinkmann AO, et al. Distinct functional differences of human progesterone receptors A and B on gene expression and growth regulation in two endometrial carcinoma cell lines. *Journal of the Society for Gynecologic Investigation*. 2003; 10:49–57. [PubMed: 12517594]
12. Kandoth C, Schultz N, Cherniack AD, Akbani R, Liu Y, et al. Cancer Genome Atlas Research N. Integrated genomic characterization of endometrial carcinoma. *Nature*. 2013; 497:67–73. [PubMed: 23636398]

13. Gu C, Zhang Z, Yu Y, Liu Y, Zhao F, Yin L, et al. Inhibiting the PI3K/Akt pathway reversed progesterin resistance in endometrial cancer. *Cancer science*. 2011; 102:557–564. [PubMed: 21205080]
14. Pant A, Lee II, Lu Z, Rueda BR, Schink J, Kim JJ. Inhibition of AKT with the orally active allosteric AKT inhibitor, MK-2206, sensitizes endometrial cancer cells to progesterin. *PloS one*. 2012; 7:e41593. [PubMed: 22911820]
15. Clarke CL, Graham JD. Non-overlapping progesterone receptor cistromes contribute to cell-specific transcriptional outcomes. *PLoS One*. 2012; 7:e35859. [PubMed: 22545144]
16. Mohammed H, D'Santos C, Serandour AA, Ali HR, Brown GD, Atkins A, et al. Endogenous purification reveals GREB1 as a key estrogen receptor regulatory factor. *Cell reports*. 2013; 3:342–349. [PubMed: 23403292]
17. Bergers G, Benjamin LE. Tumorigenesis and the angiogenic switch. *Nature reviews Cancer*. 2003; 3:401–410. [PubMed: 12778130]
18. Daikoku T, Hirota Y, Tranguch S, Joshi AR, DeMayo FJ, Lydon JP, et al. Conditional loss of uterine Pten unfaithfully and rapidly induces endometrial cancer in mice. *Cancer research*. 2008; 68:5619–5627. [PubMed: 18632614]
19. Rubel CA, Lanz RB, Kommagani R, Franco HL, Lydon JP, DeMayo FJ. Research resource: Genome-wide profiling of progesterone receptor binding in the mouse uterus. *Mol Endocrinol*. 2012; 26:1428–1442. [PubMed: 22638070]
20. Takano M, Lu Z, Goto T, Fusi L, Higham J, Francis J, et al. Transcriptional cross talk between the forkhead transcription factor forkhead box O1A and the progesterone receptor coordinates cell cycle regulation and differentiation in human endometrial stromal cells. *Mol Endocrinol*. 2007; 21:2334–2349. [PubMed: 17609436]
21. Vasquez YM, Mazur EC, Li X, Kommagani R, Jiang L, Chen R, et al. FOXO1 is required for binding of PR on IRF4, novel transcriptional regulator of endometrial stromal decidualization. *Mol Endocrinol*. 2015; 29:421–433. [PubMed: 25584414]
22. Goto T, Takano M, Albergaria A, Briese J, Pomeranz KM, Cloke B, et al. Mechanism and functional consequences of loss of FOXO1 expression in endometrioid endometrial cancer cells. *Oncogene*. 2008; 27:9–19. [PubMed: 17599040]
23. Aitken A. 14-3-3 proteins: a historic overview. *Seminars in cancer biology*. 2006; 16:162–172. [PubMed: 16678438]
24. Quayle SN, Sadar MD. 14-3-3 sigma increases the transcriptional activity of the androgen receptor in the absence of androgens. *Cancer Lett*. 2007; 254:137–145. [PubMed: 17433535]
25. Titus MA, Tan JA, Gregory CW, Ford OH, Subramanian RR, Fu H, et al. 14-3-3{eta} Amplifies Androgen Receptor Actions in Prostate Cancer. *Clin Cancer Res*. 2009; 15:7571–7581. [PubMed: 19996220]
26. Wakui H, Wright AP, Gustafsson J, Zilliacus J. Interaction of the ligand-activated glucocorticoid receptor with the 14-3-3 eta protein. *J Biol Chem*. 1997; 272:8153–8156. [PubMed: 9079630]
27. Zilliacus J, Holter E, Wakui H, Tazawa H, Treuter E, Gustafsson JA. Regulation of glucocorticoid receptor activity by 14--3-3-dependent intracellular relocalization of the corepressor RIP140. *Mol Endocrinol*. 2001; 15:501–511. [PubMed: 11266503]
28. De Vries-van Leeuwen IJ, da Costa Pereira D, Flach KD, Piersma SR, Haase C, Bier D, et al. Interaction of 14-3-3 proteins with the estrogen receptor alpha F domain provides a drug target interface. *Proc Natl Acad Sci U S A*. 2013; 110:8894–8899. [PubMed: 23676274]
29. Lodygin D, Diebold J, Hermeking H. Prostate cancer is characterized by epigenetic silencing of 14-3-3sigma expression. *Oncogene*. 2004; 23:9034–9041. [PubMed: 15489902]
30. Nakayama H, Sano T, Motegi A, Oyama T, Nakajima T. Increasing 14-3-3 sigma expression with declining estrogen receptor alpha and estrogen-responsive finger protein expression defines malignant progression of endometrial carcinoma. *Pathology international*. 2005; 55:707–715. [PubMed: 16271083]
31. Mhawech P, Benz A, Cerato C, Greloz V, Assaly M, Desmond JC, et al. Downregulation of 14-3-3sigma in ovary, prostate and endometrial carcinomas is associated with CpG island methylation. *Mod Pathol*. 2005; 18:340–348. [PubMed: 15257317]

32. Winter S, Simboeck E, Fischle W, Zupkovitz G, Dohnal I, Mechtler K, et al. 14-3-3 proteins recognize a histone code at histone H3 and are required for transcriptional activation. *EMBO J*. 2008; 27:88–99. [PubMed: 18059471]
33. Razandi M, Pedram A, Levin ER. Estrogen signals to the preservation of endothelial cell form and function. *J Biol Chem*. 2000; 275:38540–38546. [PubMed: 10988297]
34. Gibson DA, Greaves E, Critchley HO, Saunders PT. Estrogen-dependent regulation of human uterine natural killer cells promotes vascular remodelling via secretion of CCL2. *Hum Reprod*. 2015; 30:1290–1301. [PubMed: 25820695]
35. Shifren JL, Tseng JF, Zaloudek CJ, Ryan IP, Meng YG, Ferrara N, et al. Ovarian steroid regulation of vascular endothelial growth factor in the human endometrium: implications for angiogenesis during the menstrual cycle and in the pathogenesis of endometriosis. *J Clin Endocrinol Metab*. 1996; 81:3112–3118. [PubMed: 8768883]
36. Hsu SP, Ho PY, Juan SH, Liang YC, Lee WS. Progesterone inhibits human endothelial cell proliferation through a p53-dependent pathway. *Cellular and molecular life sciences: CMLS*. 2008; 65:3839–3850. [PubMed: 18850315]
37. Lebovic DI, Shifren JL, Ryan IP, Mueller MD, Korn AP, Darney PD, et al. Ovarian steroid and cytokine modulation of human endometrial angiogenesis. *Hum Reprod*. 2000; 15(Suppl 3):67–77. [PubMed: 11041223]
38. Okada H, Okamoto R, Tsuzuki T, Tsuji S, Yasuda K, Kanzaki H. Progestins inhibit estradiol-induced vascular endothelial growth factor and stromal cell-derived factor 1 in human endometrial stromal cells. *Fertil Steril*. 2011; 96:786–791. [PubMed: 21774929]
39. Goddard LM, Murphy TJ, Org T, Enciso JM, Hashimoto-Partyka MK, Warren CM, et al. Progesterone receptor in the vascular endothelium triggers physiological uterine permeability preimplantation. *Cell*. 2014; 156:549–562. [PubMed: 24485460]
40. Livak KJ, Schmittgen TD. Analysis of relative gene expression data using real-time quantitative PCR and the 2^{−(Delta Delta C(T))} Method. *Methods*. 2001; 25:402–408. [PubMed: 11846609]
41. Sefton EC, Qiang W, Serna V, Kurita T, Wei JJ, Chakravarti D, et al. MK-2206, an AKT inhibitor, promotes caspase-independent cell death and inhibits leiomyoma growth. *Endocrinology*. 2013; 154:4046–4057. [PubMed: 24002033]

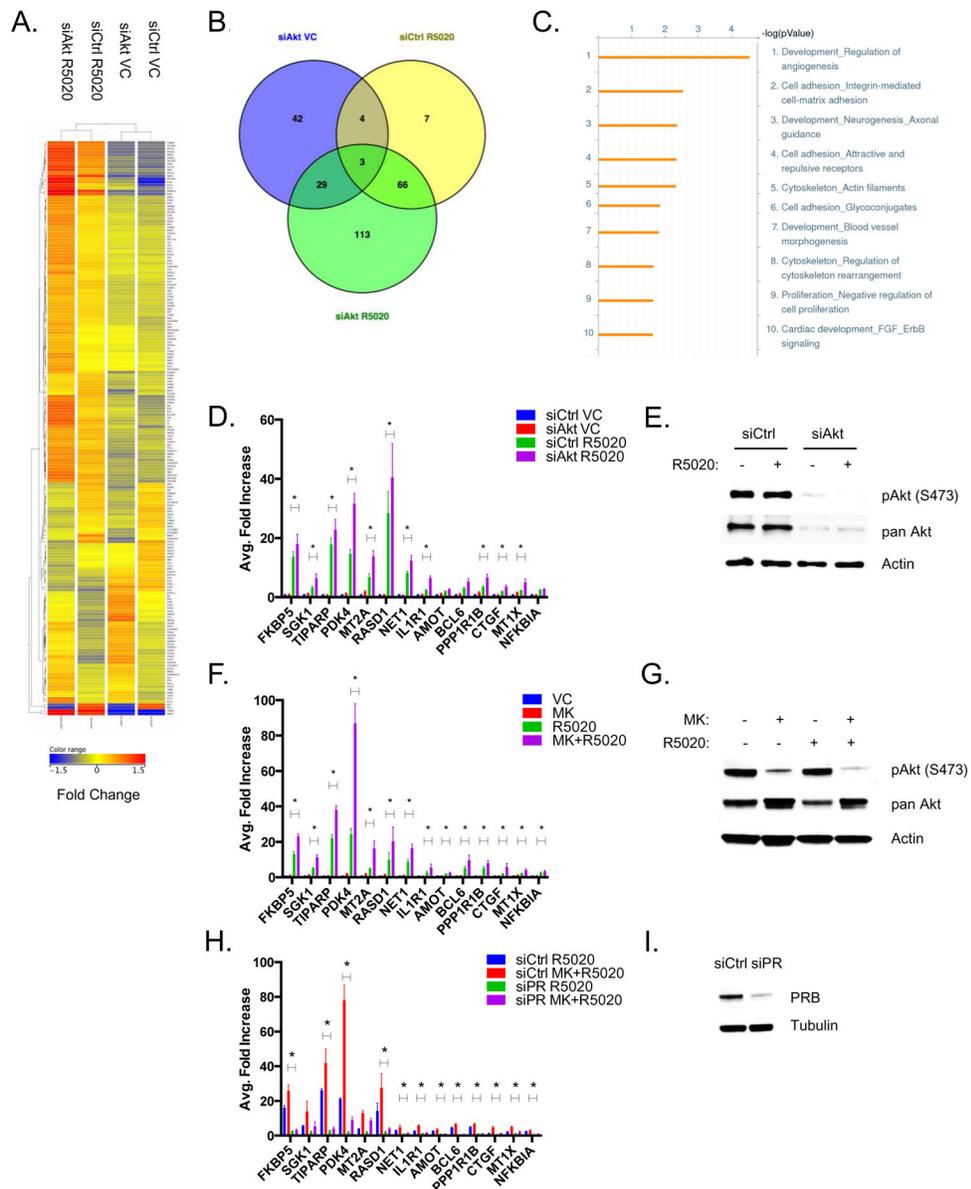


Figure 1. Knockdown or inhibition of Akt activity upregulates PRB transcriptional activity
 A) PRB-Ishikawa cells were transfected with either siCtrl or siAkt1-3. Following transfection, cells were serum-starved and then treated with either Ethanol Vehicle or 10 nM R5020 for 24 hrs. RNA was extracted and microarray analysis was performed. Heatmap analysis was performed to display the differentially expressed genes. B) Venn Diagram showing the distribution and overlap of differentially expressed genes in the siAkt Vehicle, siCtrl R5020, and siAkt R5020 datasets. C) Gene ontology analysis using GeneGO was performed to determine the key processes enriched in the siAkt R5020 differentially expressed dataset. D) PRB-Ishikawa cells were transfected with either siCtrl or siAkt1-3. Following transfection, cells were serum-starved and then treated with either Vehicle, or 10 nM R5020 for 24 hrs. RNA was extracted and real-time PCR analysis was performed. E) Whole cell protein lysates were also extracted and phospho Akt (S473), pan Akt, and Actin

were detected by western blotting. F) PRB-Ishikawa cells were serum-starved overnight and then treated with either DMSO and Ethanol Vehicle, 1 μ M MK-2206, 10 nM R5020, or 1 μ M MK-2206 + 10 nM R5020 for 24 hrs. RNA was extracted and real-time PCR analysis was performed. G) Whole cell lysates were also extracted and phospho Akt (S473), pan Akt, and Actin were detected by western blotting. H) PRB-Ishikawa cells were transfected with either siCtrl or siPR. Following transfection, cells were serum-starved and then treated with either Vehicle, 1 μ M MK-2206, 10 nM R5020, 1 μ M MK-2206 + 10 nM R5020 for 24 hrs. RNA was extracted and real-time PCR was performed. I) Whole cell lysates were also extracted and PR and Tubulin were detected by western blotting. Error bars represent SEM of three independent experiments, and * $p < 0.05$.

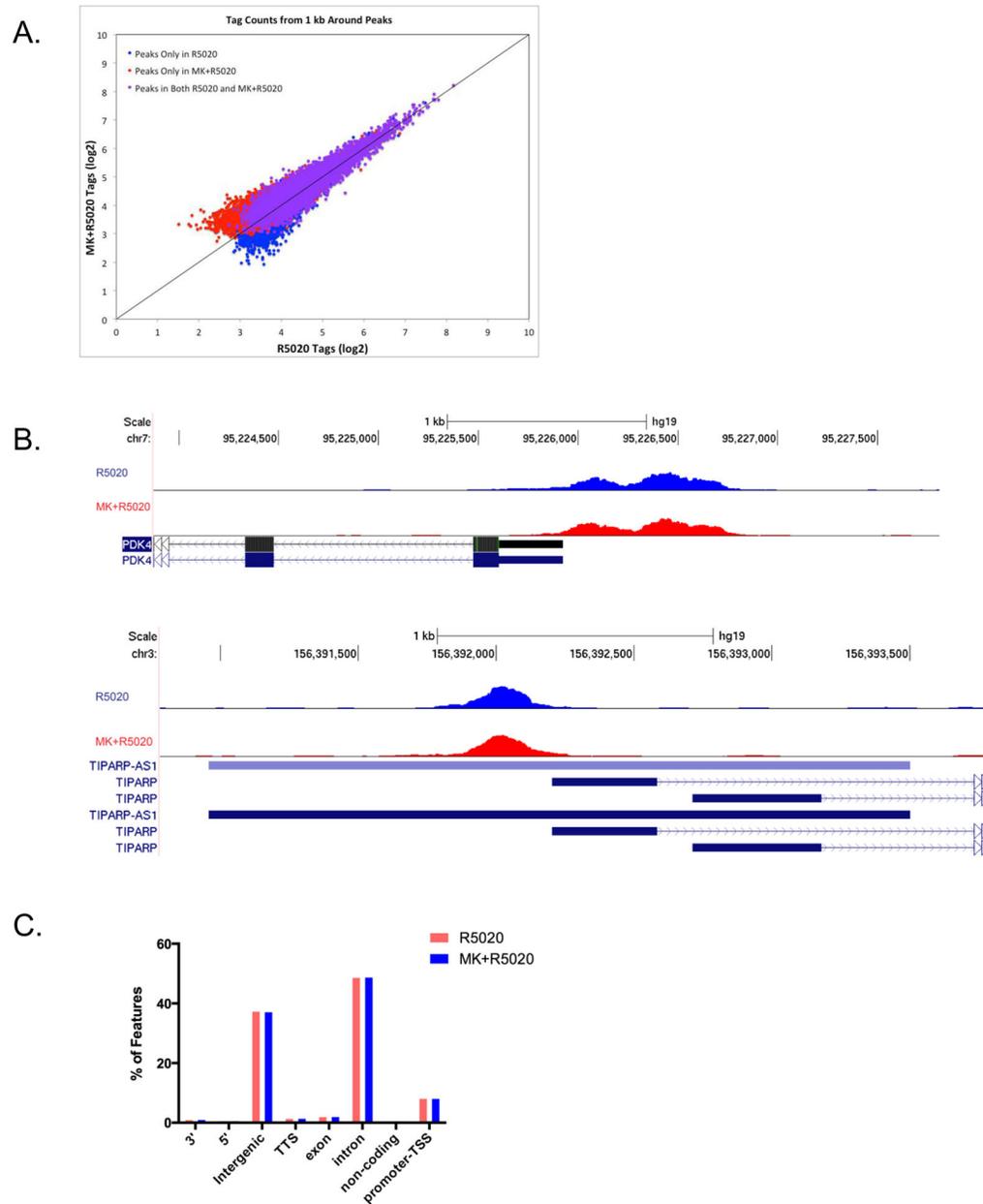


Figure 2. ChIP-Seq Analysis indicates that inhibition of Akt does not alter PRB genome-wide recruitment

A) PRB-Ishikawa cells were serum-starved overnight and then pre-treated with either DMSO Vehicle Control or 1 μ M MK-2206 overnight. After pre-treatment, cells were treated with 10 nM R5020 for 30 minutes. Tag density counts for the R5020 treatment were plotted against the tag density counts for the MK+R5020 treatment. B) UCSC Genome Browser visualization of the *PDK4* and *TIPARP* gene regions. R5020 treatment (blue peaks), MK+R5020 treatment (red peaks). C) R5020 and MK+R5020 peaks were annotated and the distribution of PR-binding regions was displayed.

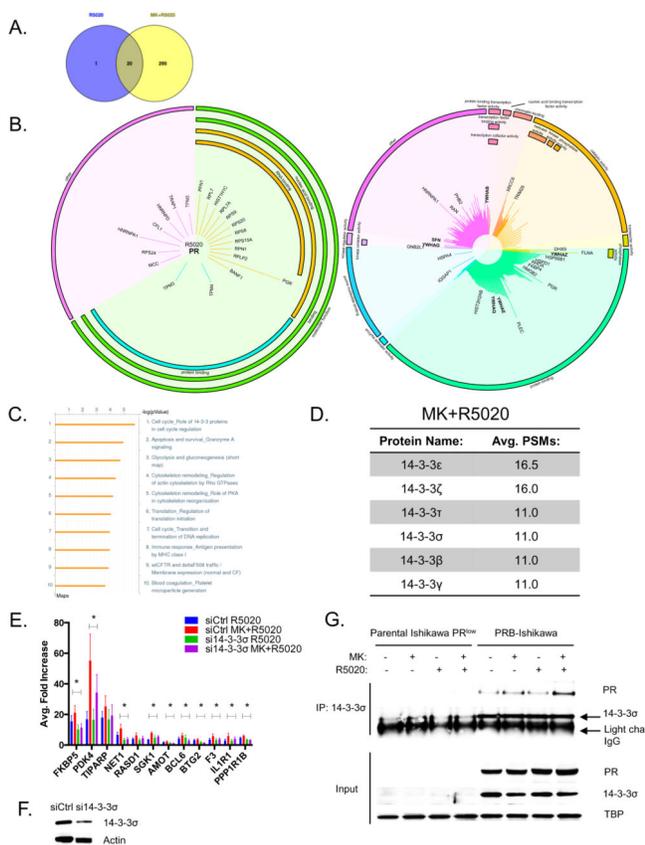


Figure 3. ChIP-Mass Spectrometry Analysis identifies 14-3-3σ is required for the induction in PRB target genes following Akt inhibition

PRB-Ishikawa cells were serum-starved overnight and then pre-treated with either DMSO Vehicle Control or 1 μM MK-2206 overnight. After pre-treatment, cells were treated with 10 nM R5020 for 30 minutes. A) Venn Diagram showing the distribution and overlap of the identified proteins in the R5020 and MK+R5020 datasets. B) Graphical plot (MS-ARC) displaying proteins identified in the R5020 and MK+R5020 datasets. Proteins are grouped according to gene ontology terms and the length of the line corresponds to the average PSMs. 14-3-3 family members are in bold. C) Gene Ontology analysis using GeneGO displays the enriched pathways in the MK+R5020 dataset. D) Table displaying the 14-3-3 family members identified in the MK+R5020 dataset with their corresponding average PSMs. E) PRB-Ishikawa cells were transfected with either siCtrl or si14-3-3σ. Following transfection, cells were serum-starved and then treated with either DMSO and Ethanol Vehicle, 1 μM MK-2206, 10 nM R5020, 1 μM MK-2206 + 10 nM R5020 for 24 hrs. RNA was extracted and real-time PCR was performed. F) Protein lysates were also extracted and subjected to western blot analysis and 14-3-3σ and Actin were detected. Error bars represent SEM of three independent experiments, and *p < 0.05. G) Parental Ishikawa PR^{low} and PRB-Ishikawa cells were serum-starved and then pre-treated with either DMSO Vehicle Control or 1 μM MK-2206 overnight. After pre-treatment, cells were treated with either Ethanol Vehicle, or 10 nM R5020 for 30 minutes. After treatment, cells were harvested,

nuclear extracts were prepared, and were immunoprecipitated with 14-3-3 σ . Immunoprecipitates were analyzed by western blotting and PR and 14-3-3 σ were detected.

Author Manuscript

Author Manuscript

Author Manuscript

Author Manuscript

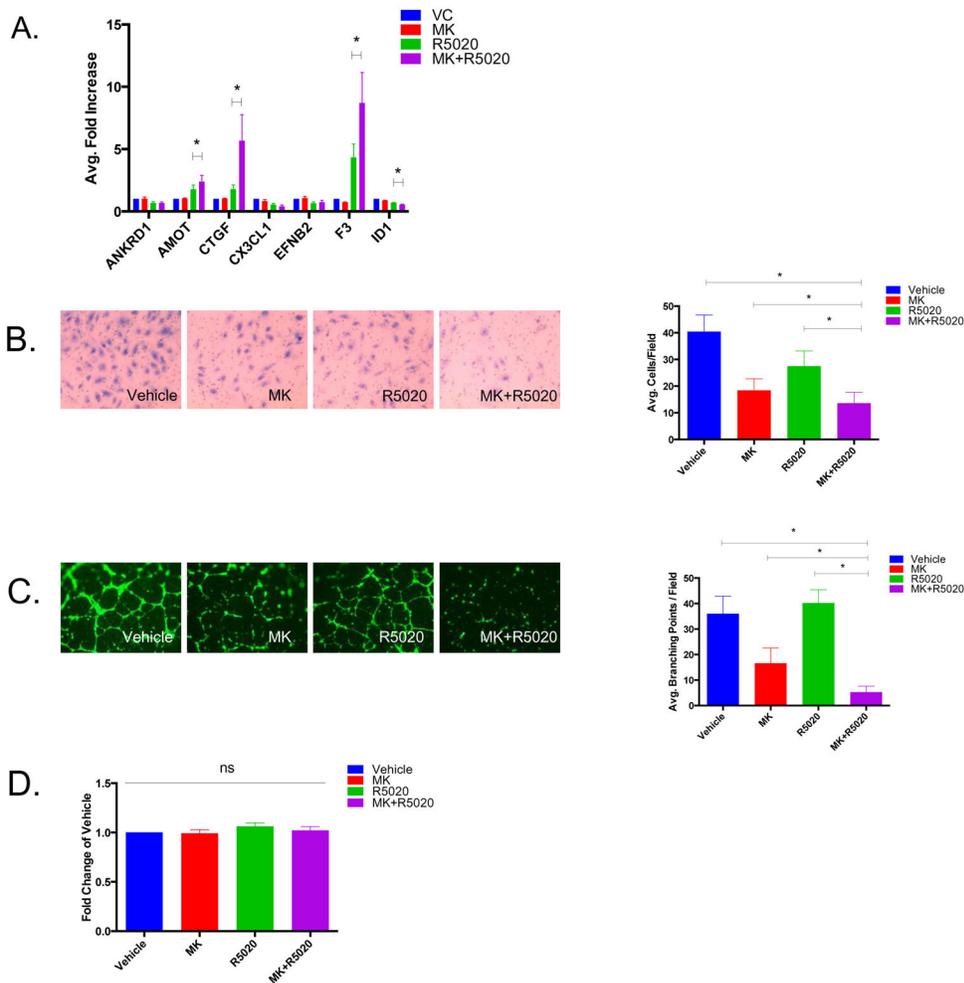


Figure 4. Combinatorial MK+R5020 treatments further decrease angiogenesis in vitro
 A) PRB-Ishikawa cells were serum-starved overnight and then treated with either DMSO and Ethanol Vehicle, 1 μ M MK-2206, 10 nM R5020, or 1 μ M MK-2206 + 10 nM R5020 for 24 hrs. RNA was extracted and real-time PCR analysis was performed. B) An endothelial invasion assay was performed using Uterine Microvascular Epithelial Cells (UtMVEC) and conditioned media from PRB-Ishikawa cells treated with either DMSO and Ethanol Vehicle, 1 μ M MK-2206, 10 nM R5020, or MK+R5020 for 24 hrs. Invasive UtMVEC cells were then stained and counted by microscopy. C) An endothelial tube formation assay was performed using UtMVEC and conditioned media from PRB-Ishikawa cells treated with either DMSO and Ethanol Vehicle, 1 μ M MK-2206, 10 nM R5020, or MK+R5020 for 24 hrs. Cells were then stained with Calcein AM and photographs were taken using immunofluorescence microscopy; branching points were quantified. D) A WST cell viability assay was performed on UtMVEC cells treated with conditioned media from PRB-Ishikawa cells treated with either DMSO and Ethanol Vehicle, 1 μ M MK-2206, 10 nM R5020, or MK+R5020 for 24 hrs. Error bars represent SEM of three independent experiments, * $p < 0.05$.

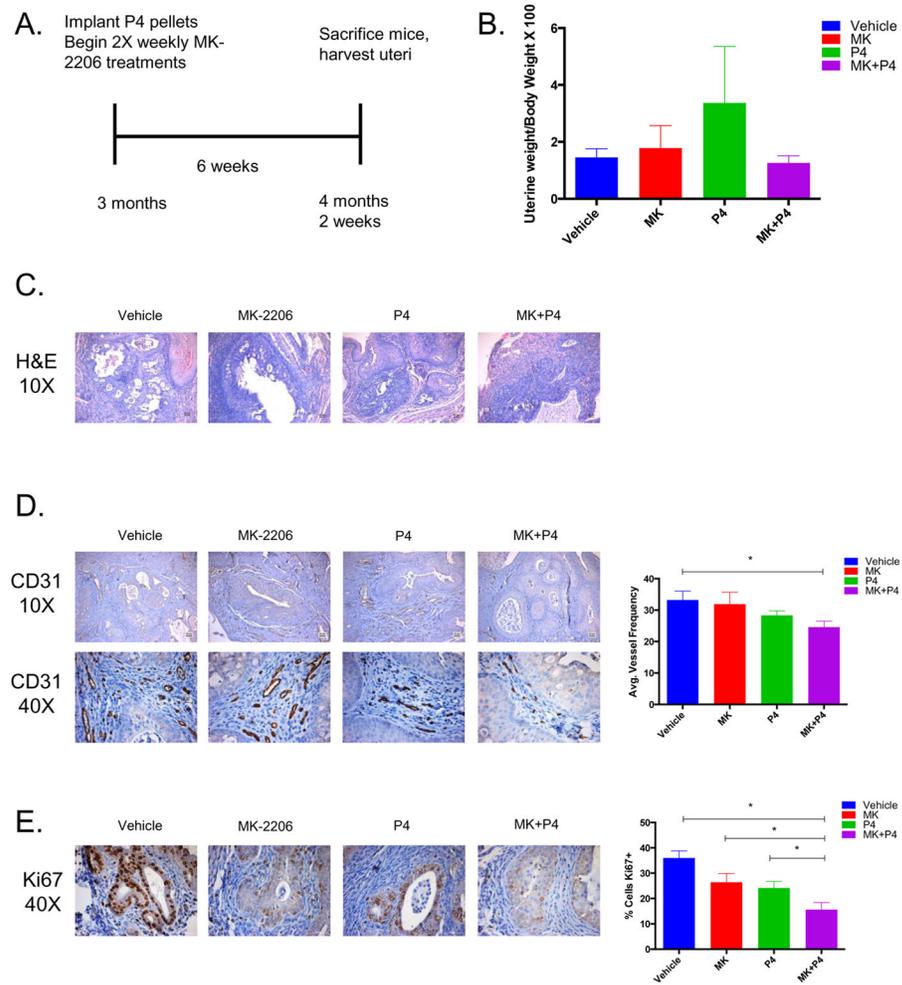


Figure 5. Combinatorial MK-2206 and Progesterone treatments further decrease angiogenesis and proliferation in a conditional uterine *PTEN*^{d/d} mouse model

A) Treatment overview of *PTEN*^{d/d} mice. B) Ratio of uterine weight to total body weight was measured for each of the Vehicle, MK-2206, P4, and MK+P4 treatment groups. C) H&E staining was performed on tissue sections from the Vehicle, MK-2206, P4, and MK+P4 treatment groups (10X magnification). D) CD31 staining was performed on tissue sections from the Vehicle, MK-2206, P4, and MK+P4 treatment groups (10X, 40X magnifications). CD31 staining was quantified using ImageJ. E) Ki67 staining was performed on tissue sections from the Vehicle, MK-2206, P4, and MK+P4 treatment groups (40X magnification). Ki67 staining was quantified using ImageJ.

Table 1
HOMER Enriched Motifs in the R5020 and MK+R5020 treatments

The top twelve enriched HOMER motifs identified in PR-ChIP Seq in the R5020 and MK+R5020 datasets.

Rank	Motif (R5020)	Motif (MK+R5020)
1	PRE	PRE
2	GRE	GRE
3	ARE	ARE
4	GRE	GRE
5	AR Half Site	AR Half Site
6	Fra1	Fra1
7	Jun-AP1	Fosl2
8	Fosl2	Jun-AP1
9	BATF	BATF
10	Atf3	Atf3
11	AP-1	AP-1
12	NF1	NF1

Author Manuscript

Author Manuscript

Author Manuscript

Author Manuscript

Table 2**PTEN^{d/d} mouse uterine histology**

PTEN d/d uterine tissues were stained with H&E and scored by a pathologist according to FIGO guidelines for endometrial cancer grading.

	Vehicle (# mice) N=9	MK-2206 (# mice) N=9	P4 (#mice) N=9	MK+P4 (# mice) N=10
Benign squamous metaplasia	0	1	1	4
Grade I endometrioid carcinoma	1	1	0	2
Grade I endometrioid carcinoma with squamous metaplasia	7	3	6	3
Grade I endometrioid carcinoma with malignant squamous metaplasia	1	0	0	0
Grade II endometrioid carcinoma with squamous metaplasia	0	4	2	1

Author Manuscript

Author Manuscript

Author Manuscript

Author Manuscript